Journal Name

ARTICLE

Intermatrix Synthesis of Ag, AgAu and Au nanoparticles by Galvanic Replacement Strategy for bactericidal and electrocatalytically active nanocomposites

Received 00th January 20xx,
Accepted 00th January 20xx

DOI: 10.1039/x0xx00000x

www.rsc.org/

Julio Bastos-Arrieta[a]*, Jose Muñoz[b], Núria Vigués[c], Dmitri N. Muraviev[d], Francisco Céspedes[d], Jordi Mas[c], Mireia Baeza[d] and Maria Muñoz[d]

Intermatrix Synthesis technique (IMS) has proven to be an environmentally friendly methodology for the preparation of functional metal nanoparticles (FMNPs) on different reactive matrices. The distribution of these FMNPs is an important feature to control depending on the final application of the Nanocomposite: bactericide assays for water treatment, heterogeneous catalysis, electrocatalytical effects and others. IMS offers the feasibility to control the FMNPs distribution, taking into account the adequacy of the ion exchange form of the reactive matrix and the chemical nature of the reducing agent used for the synthesis (Donnan Effect). Consequently, AgAu–FMNPs and Au–FMNPs containing nanocomposites have been prepared by coupling a galvanic replacement stage to IMS, with tested bactericide features attributed to the distribution of the nanoparticles on the material. In addition, Ag–FMNPs and Au–FMNPs contained on multiwalled carbon nanotubes have been synthesized and used as conducting nanofillers for the development of amperometric nanocomposite sensors based on epoxy resin. The incorporation of these FMNPs on the nanocomposite sensor has shown signficant electrocatalytical effects, obtaining enhanced electrochemical and analytical parameters, such as higher signal-to-noise ratios as well as better detection limits, quantification limits and sensitivities for the oxidation of ascorbic acid in water, which was used as a model analyte

Introduction

Recently, the development of efficient green chemistry methods for synthesis of nanostructured materials (including nanoparticles (NPs), nanowires and carbon nanotubes (CNTs))[1–4] have been intensively investigated due to their size related features, special chemical and physical properties[5]. This makes relevant their incorporation into hybrid nanocomposite materials with potential application for electronic, optical and magnetic devices.

One mayor feature to take into account of these novel added value materials is the distribution of the Functional Metal Nanoparticles (FMNPs) in terms of size and matrix location, space, physical and chemical properties of the matrix formed, and the understanding of the kinetics of the joint FMNPs-matrix system. Moreover, it is important to consider the affinity of the FMNPs and adhesion to the matrix and the possible consequent changes of the matrix (porosity, ion exchange capacity).[6,7]

FMNPs distribution in composite materials is of great importance when considering their feasible further applications. For example, in catalytic applications,[8] the best situation is when the catalysts FMNPs are located near the supporting matrix surface what provides the maximum accessibility of the reactants to the catalytic centres. In electrochemical or electroanalytical applications (e.g., in (bio)sensors), a homogeneous distribution of FMNPs has been considered to be preferable as it enhances the electron conductivity of the system.[9,10] Accordingly, electrodes based on modified CNTs with these FMNPs have shown excellent electrocatalytic activity because of the fast electron transfer ability of CNTs, as can be seen in the electrochemical detection of hydrogen peroxide, glucose and ascorbic acid[11–13]. Under this context, FMNPs have received considerable attention for their catalytic and electrochemical features for the preparation of amperometric sensors and biosensors, leading to an enhancement of the electron transfer between redox centres in the analyte and electrode.[14,15] Despite these advantages, the surface modification of CNTs with nanocrystals as FMNPs usually involves thermal evaporation[16], electroless deposition

[a]*Departament d'Enginyeria Química, Universitat Politècnica de Catalunya (UPC), Campus Diagonal Besòs, Edificio C (EEBE). Carrer Eduard Maristany, 10-14. 08019, Barcelona, Spain*
[b]*Molecular Nanoscience and Organic Materials Group, Institut de Ciència de Materials de Barcelona (ICMAB-CSIC) Campus UAB, 08193 Bellaterra, Spain*
[c]*Department of Genetics and Microbiology, Universitat Autònoma de Barcelona 08193 Cerdanyola del Vallès (Bellaterra), Spain.*
[d]*Departament de Química, Facultat de Ciències, Edifici C-Nord, Universitat Autònoma de Barcelona, 08193 Cerdanyola del Vallès (Bellaterra), Spain.*
**Corresponding author: Dr. Julio Bastos-Arrieta julio.bastos@upc.edu*
Electronic Supplementary Information (ESI) available: ESI.1: contains size distribution histograms for Au-Nanoparticles. ESI.2: contains data of Intermatrix synthesis technique when using a neutral reducing agent. ESI.3: contains SEM images and size Distribution histograms for AgAu and Au Nanoparticles prepared by Galvanic Replacement Strategy. See DOI: 10.1039/x0xx00000x

by galvanic replacement[17], MNPs hydrosol absorption[18] or electrochemical deposition.[19]

Intermatrix Synthesis (IMS) is an *in situ* methodology for the preparation of nanocomposite materials (NCs) mainly used in different reactive matrices with ion exchange properties[20]. The main features of IMS make it suitable for the modification of all types of matrices (polymeric or not) with ion exchange functionality and for different types of NPs. The main requirements for an ion exchange matrix to be used as a support for the IMS technique include:[21,22]

- The matrix must be chemically compatible with the NPs surface.
- It bears a charge due to the presence of well-dissociated functional ion exchange groups. This requires a preconditioning acid –base and NaCl treatment of the supporting matrix before IMS technique that usually results in the Na^+-form for cationic exchangers and the Cl^--form for anionic
- Appropriate distances between the functional groups, in order to avoid agglomeration of FMNPs due to steric effects on the surface.

IMS is based on the Donnan Effect (DE) interaction between FMNPs precursors and the reactive matrix. DE acts as driven force of the final distribution of the nanoparticles[23–26], which can be tailored considering the general stages of classical IMS[9,10,21,25,27]

a) Loading of the matrix with the desired FMNPs precursor cations and achieve their immobilization (sorption) onto the functional groups.
b) Chemical reduction to zero-valent FMNPs with the appropriate reducing agent.

Thus, depending on the selection of charged reducing agent, Donnan Effect (DE) for both cation exchange and anion exchange matrices; results in the formation mainly near the surface of the matrix. If a neutral reducing agent is chosen, the location of the FMNPs in the final material is in both the interior and exterior zone of the matrix. In addition, a symmetrical version of IMS can be achieved, when the reducing agent is fixed in the matrix during the initial stage with the consequent loading of the FMNPs precursor. This extension of IMS resulted suitable for the preparation of Pd nanocatalysts on anion exchange polymeric beads[10]. Moreover, one advantage of IMS can be observed after the formation of the NPs with tuned distribution, the initial ion exchange functionality is recovered and then, the ion exchange capacity of the supporting matrix is not significantly changed due to IMS[28].

This communication presents the slight modification of IMS by incorporating a galvanic replacement stage. Galvanic replacement reaction takes place due to the difference in half-cell potentials between the metal ions to be reduced and the substrate to be oxidized[29,30]. This is the case for Ag and Au. The synthesis of Au-FMNPs composites is interesting due to their well-known electrochemical properties[31,32] and their feasible application for bactericide assays[33,34]. The use of Au nanomaterials as bactericidal agents represents a novel paradigm in the development of therapeutics against drug-resistant pathogenic bacteria[33]**.** Therefore, in order to obtain Au-FMNPs mainly located on the surface of a polymeric bead, the incorporation of a galvanic stage in IMS was implemented.. These NCs have been successfully tested in bactericide assays.
Finally, IMS has also been applied for the preparation of electrocatalytic active nanocomposites for sensing purposes. For this aim, CNTs were modified with Ag-FMNPs and Au-FMNPs and used as conducting nanofiller materials in an insulating polymeric matrix (the epoxy resin) for amperometric purposes. After electrochemical and electroanalytical experiments, the developed nanocomposite sensors exhibited significant enhancements in several analytical parameters for ascorbic acid determination, which was used as a model analyte.

Experimental

Materials and Reagents

Metal salts (NaBH4, HAuCl4, AgNO3,) from Sigma Aldrich were of p.a. grade were used as received. All dissolutions were prepared using deionised water from a Milli-Q system (Millipore, Billerica, MA, USA. A520E anion exchange resinswere supplied by Purolite® (Purolite Iberica S.I., Barcelona, Spain). All reagents were of the highest grade available and used without further purification. Raw multiwalled carbon nanotubes (MWCNTs) were provided by SES Research (Houston, TX, USA) whose physical properties are > 95% of carbon purity, 10–30 nm of outer diameter and 5–15 μm of length. They were produced using chemical vapor deposition (CVD) method. Epotek H77A and its corresponding hardener Epotek H77B were obtained from Epoxy Technology (Billerica, MA, USA) and were used as polymeric matrix.

Synthesis of Ag, AgAu and Au-FMNPs on gel-type anion exchange resin by IMS technique

The synthesis of Ag-FMNPs was carried out by the loading the functional groups of the anion exchanger Purolite® A520E resin, with anions of the reducing agent using 20 mL 0.5 mol·L-1 aqueous solution NaBH4 followed by the treatment of the resin with 20 mL 0.1 mol·L-1 AgNO3 solution. The last stage resulted in the formation of the Ag-FMNPs mainly on the surface of the polymer matrix.

The preparation of AgAu-FMNPs nanocomposite was carried out by adding 10 mL of 0.01 mol·L-1 aqueous HAuCl4 solution to previously prepared Ag-NPs containing nanocomposite, with the consequent galvanic replacement of Au to Ag; which under these conditions and amounts of reagents, lead to obtain hybrid AgAu nanocomposites.

Finally, the preparation of Au-NPs composites with was carried out as well by galvanic replacement stage, by adding 15.7 mL of 0.01 mol·L-1 aqueous HAuCl4 solution in order to obtain the total exchange of Au to Ag mainly on the surface of the polymer bead. In all cases, the final NC material was rinsed three times with deionized water.

Synthesis of Ag-FMNPs and Au-FMNPs on multiwalled carbon nanotubes by IMS technique and electrodes preparation

Firstly, the MWCNTs surface was activated with carboxylic groups by 2.5 M nitric acid treatment in ultrasound bath for 2 h and then, the carboxylic groups on the MWCNTs were converted to Na+ form by their immersion in 1.0 M NaCl solution with mechanical stirring, as shown in Equation (1).

$$[MWCNTs–COO^- H^+] + Na^+ \rightarrow [MWCNTs–COO^- Na^+] + H^+ \quad (1)$$

Afterwards, the synthesis of Ag-FMNPs and Au-FMNPs on MWCNTs surface was carried out by IMS technique resulting the hybrid-nanomaterials Ag-FMNPs@MWCNTs and Au-FMNPs. IMS can be described as follows:

Stage 1: Loading of Mn+ ions (e.g., Ag+ metal precursors) onto the carboxylic groups of MWCNTs, see Equation (2).

$$[MWCNTs–COO^- Na^+] + Ag^+ \rightarrow [MWCNTs–COO^-] Ag^+ + Na^+ \quad (2)$$

Stage 2: Formation of the FMNPs on the MWCNTs surface by adding the NaBH4 reducing agent, see Equation (3).

$$[MWCNTs–COO^-] Ag^+ + Na^+ BH_4^- \rightarrow [MWCNTs–COO^- Na^+] Ag\text{-}FMNPs\downarrow + ½ H_2 + B(OH)_3 \quad (3)$$

Having synthesized the hybrid-nanomaterials, they were used as conducting nanofillers for electrodes construction. Handmade working nanocomposite electrodes were prepared by mixing polymer Epotek H77A and its corresponding H77B hardener in a 20:3 (w/w) ratio and adding 10% (w/w) of either raw MWCNTs or FMNPs@MWCNTs, which was found as the optimum filler/polymer composition ratio.35 The nanofiller materials were dispersed through the polymeric matrix and hardener agents by manually homogenization for 1h following the methodology previously described in our research group32. The final electrode dimensions were 28 mm2 of physic area.

Finally, it is important to highlight that the raw MWCNTs were also activated with carboxylic groups following the Equation (1) due to they were used as a blank for the characterization studies.

Analysis of metal content by Induced Coupled Plasma (ICP)

A sample of about 10 mg of NCs material was immersed in aqua regia (1 mL) to completely dissolve the metals by oxidation. The solution was filtered through a 0.22 µm Millipore filter and diluted for metal content quantification by ICP-MS (Agilent 7500). The average uncertainty of metal ions determination was less than 2% in all cases.

Evaluation of Bacteria Inhibitory Activity

Different amounts of nanocomposite bead with different Au content, were placed in contact with E. coli K12 (1e3 cfu/mL) overnight at 37 ºC. Absorbance measurements (3 replicates) were taken at 650nm in a Thermo Electron Multiskan EX plate reader (VWR International, Pennsylvania)

Electron Microscopy Characterisation

Field Emission Scanning Electron Microscopy (FE-SEM) coupled with an Energy-Dispersive Spectrometer (EDS) Zeiss® MERLIN from Servei de Microscopia of Universitat Autonoma de Barcelona was used for SEM pictures The NCs samples were prepared by embedding several granules in the epoxy resin followed by cutting with an ultramicrotome (Leica EM UC6, Leica Microsystems Ltd., Milton Keynes, UK) using a 35° diamond knife (Diatome, Hatfield, PA, USA) at liquid nitrogen temperature (−160 °C). EDS spectra combined with -SEM evidence the distribution profile of FMNPs in the NCs.

For the characterization of MWCNT-based samples (containing or not FMNPS), experiments were carried out using a High Resolution Transmission Electron Microscopy (HR-TEM) coupled to an EDS (JEM-1400 unit with an acceleration voltage of 120 kV). Approximately 1 mg of sample was dispersed in 5 mL of acetone as organic solvent and then placed in ultrasound bath for 1h. Finally, a drop of the solution was placed on a grid and it was dried before HR-TEM analysis.

FMNPs content in MWCNTs by thermogravimetric analysis

Thermogravimetric analysis (TGA) were performed on a Netzsch instrument, model STA 449 F1 Jupiter® (Selb, Bavaria, Germany), with a flow of air. ~ 20 mg sample was heated to 1000 ºC at 10 ºC/min, using air flow. The mass of the sample was continuously measured as a function of temperature and the rate of weight loss (d.t.g.) was automatically recorded.

Electrochemical and electroanalytical experiments

Cyclic Voltammetry (CV) and Electrochemical Impedance Spectroscopy (EIS) measurements were performed using a computer controlled Autolab PGSTAT30 potentiostat/galvanostat (EcoChemie, Utrech, The Netherlands) using GPES (v.4.9) software package provided by the manufacturer. A three electrode configuration cell was used for impedimetric and voltammetric measurements. An AgCl covered silver wire reference electrode and a platinum-based electrode 52-671 (Crison Instruments, Alella, Barcelona, Spain) were used as reference and auxiliary electrodes, respectively. FMNPs modified and non-modified nanocomposite electrodes were used as working electrodes. EIS and CV measurements were made in a 10.0 mL of 0.1 M potassium chloride (KCl) solution containing 0.01 M potassium ferricyanide/ferrocyanide, $[Fe(CN)_6]^{3-/4-}$, under quiescent condition. The experiments were performed at room temperature (25 ºC). The impedance spectra were recorded in the frequency range 0.1 Hz to 100 kHz at the redox equilibrium potential. The signal amplitude to perturb the system was 10 mV. The scan rate used for CV experiments was 10 $mV \cdot s^{-1}$.
Hydrodynamic amperometry measurements were made using an amperimeter LC-4C (Bio Analytical Systems INC., West Lafayette, IN, USA). A single junction reference electrode Ag/AgCl Orion 900100 (Thermo Electron Corporation, Baverly,

MA, USA) and a platinum-based electrode 52-671 were used as reference and auxiliary, respectively. MWCNT-based nanocomposite electrodes (containing FMNPs or none) were used as working electrodes. Electroanalytical measurements were carried out at fixed potential (600 mV *vs.* Ag/AgCl) under force convection by stirring the solution with a magnetic stirrer. A freshly prepared 0.10 M ascorbic acid solution was used as stock solution. Standard solutions were prepared by the dilution of the stock solution. 10.0 mL 0.01 M HNO_3/KNO_3 solution was used as a background electrolyte for ascorbic acid determination.

Results and Discussion

IMS of AgAu-FMNPs and Au-FMNPs containing NCs with favourable distribution of nanoparticles for enhanced bacteria inhibitory activity assays

The use of $HAuCl_4$, as precursor for Au-FMNPs on anion exchangers, corresponds to the loading stage of classic version of IMS is presented in equation (4). The reduction stage using $NaBH_4$ is presented in equation (5) and when using ascorbic acid as reducing agent in equation (6):

$$R\text{-}(R'_4\text{-}N)^+Cl^- + HAuCl_4 \rightarrow R\text{-}(R'_4\text{-}N)^+[AuCl_4]^- + HCl \quad (4)$$

$$R\text{-}(R'_4\text{-}N)^+[AuCl_4]^- + 3NaBH_4 + 9H_2O \rightarrow R\text{-}(R'_4\text{-}N)^+Cl^- + Au^0 + 3NaCl + 21/2H_2 + 3B(OH)_3 \quad (5)$$

$$2\ R\text{-}(R'_4\text{-}N)^+[AuCl_4]^- + 3AA \rightarrow 2\ R\text{-}(R'_4\text{-}N)^+Cl^- + Au^0 + 3\ [AA]_{ox} + 6Cl^- \quad (6)$$

The effectiveness of loading stage is evidenced by the results of Au content in the NCs. For both reducing agents, the average Au content value is 113 mg Au x g^{-1} NC. Macroscopic observation of these Au containing NCs showed a clear difference of colour: reddish for the ones prepared with $NaBH_4$ and blue for the ones prepared with ascorbic acid.

This observation is a clear example of the effect of changes caused by nanometre scale of materials. Bulk gold presents yellow colour; but when gold is subdivided into smaller and smaller particles, the ratio of the radius to the wavelength becomes important. Figure 1 presents FE-SEM images for Au-NPs synthesized by IMS using both $NaBH_4$ (Figure 1A) and ascorbic acid (Figure 1B) as reducing agents.

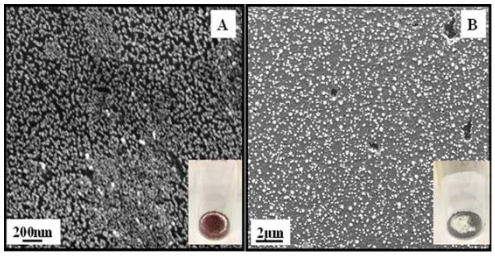

Figure 1: SEM images of Au FMNPs on anion exchanger: A) IMS using $NaBH_4$ as reducing agent. B) IMS using ascorbic acid as reducing agent. Non evidence of agglomeration is observed in neither case

The size distribution histograms show that Au-NPs synthesized with $NaBH_4$ have an average diameter of 12.0 ± 0.8 nm; meanwhile the Au-NPs synthesized with ascorbic acid have an average diameter of 79 ± 3nm (size distribution histograms can be found in ESI.1). This sizes explain the difference of macroscopic colour of the Au-NPs containing nanocomposites.

The size difference depends on the strength of the reducing agent used in the NPs formation stage, summed to the stabilization offered by the supporting matrix. A strong reducing agent ensures that the particles obtained are smaller and monodisperse than the ones obtained when using a weaker reducing agent.[36] The reduction rate of $NaBH_4$ is faster than the one from ascorbic acid. That faster rate produces a large number of NPs and may inhibit aggregation mechanisms (added to the stability offered by polymeric matrix). In order to produce larger particles, the number of NPs nuclei should be low; thus the NPs grow is related at the expense of the remaining metal ions in solutions that could be reduced.[37,38]

Cross section analysis of these NCs showed that the locations of the Au-FMNPs obtained by this IMS sequence in this anion exchange matrix, combines an interior and exterior distribution of the nanoparticles, as can be seen in figure 2. This type of location of the Au-FMNPs is not the best to obtain the best performance in feasible bactericide or catalytic effects, as has been previously reported for NCs containing Pd-FMNPs[10,26] and Ag-FMNPs[23,27,28,39] synthesized by IMS.

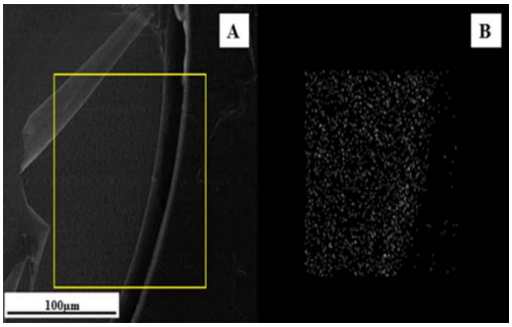

Figure 2: SEM images of Cross section of Au FMNPs in A520E resin (A) and the corresponding chemical mapping (B) of the selected square zone in yellow, showing the distribution of gold within the NC.

This can be explained by DE related with the mobility of the ions of the reducing agent selected[40,41,42]. In this case, the sign of the charge of this specie is different from the one present in the ion exchange functional groups of the supporting reactive matrix. Depending on the selection of charged reducing agent, DE for both cation exchange and anion exchange matrices; results in their formation mainly near the surface of the polymer. If a neutral reducing agent is chosen, the location of the FMNPs in the final material is distributed in the interior and exterior zone of the matrix (as presented in Electronic Supplementary Information ESI.2).

Thus, in order to obtain Au-FMNPs mainly located on the surface of this anion exchanger matrix, the galvanic replacement of Ag-FMNPs to Au-FMNPs was carried out. These Ag-FMNPs were firstly synthesized by the symmetrical version

of IMS (equations 7 and 8) with verified distribution on the surface of this resin.[39] The process consists in fixing the reducing agent BH_4^- anions and then loading the matrix with the Ag-FMNPs precursor (Ag^+). Due to DE, the cationic precursor cannot deeply penetrate into the matrix because of electrostatic repulsion (positively charged), leading to the appearance of the zero valent Ag-FMNPs mainly on the surface, as can be deducted from EDS-LineScan mapping in figure 3A and 3B.

$$R\text{-}(R_4\text{-}N)^+Cl^- + NaBH_4 \rightarrow R\text{-}(R_4\text{-}N)^+BH_4^- + NaCl \quad (7)$$

$$R\text{-}(R_4\text{-}N)\text{+}BH_4\text{-} + AgNO_3 + 3H_2O \rightarrow [R\text{-}(R_4\text{-}N)\text{+}NO_3]\ Ag^0 + 7/2\ H_2 + B(OH)_3 \quad (8)$$

Therefore, the galvanic replacement of Ag to Au which involves as well the Kinkerdall Effect, takes place in two steps: deposition of the Au on the Ag template (equation 9) and interdiffusion of atomic species of both components into the new hybrid material. During the galvanic replacement, the outward diffusion of Ag is much faster through the layer than the inward Au diffusion, as observed in EDS-LineScan mapping in figure 3C, 3D and 3E.[43] Further information about the distribution of AgAu and Au NPs on the resin surface can be found in ESI.3.

$$3Ag^0 + HAuCl \rightarrow Au^0 + HCl + 3Ag^+ \quad (9)$$

It is important to highlight that through IMS, the ion exchange functional groups of the matrix act as nanoreactors for the nucleation of the NPs; providing a confined medium for the synthesis, controlling the particle size and distribution. Moreover, the matrix itself stabilizes and isolates the generated NPs, preventing their aggregation and possible release to the medium[44].

Coupling the galvanic replacement with IMS, it results feasible to obtain bimetallic AgAu –FMNPs and monometallic Au-FMNPs nanocomposites with the FMNPs mainly located on the surface of the polymeric matrix, as it can deduct from EDS-LineScan mapping figure 3C and 3E. In addition to this fact, the metal content by ICP-MS for these samples showed that from a composite containing 245mg Ag per gram of nanocomposite, the hybrid AgAu material is composed of 85 mg Ag / 48 mg Au per gram of nanocomposite and 75mg Au per gram of nanocomposite.

Bimetallic FMNPs provide greater advantages over their monometallic counterparts, since their optical, catalytic and biological properties can be tuned by changing their composition. Au ions are reduced by Ag^0 NPs leading to the formation of an Au shell over the Ag core. In order to check feasible applications of these novel NCs, inhibitory activity tests were carried out and are presented in figure 4.

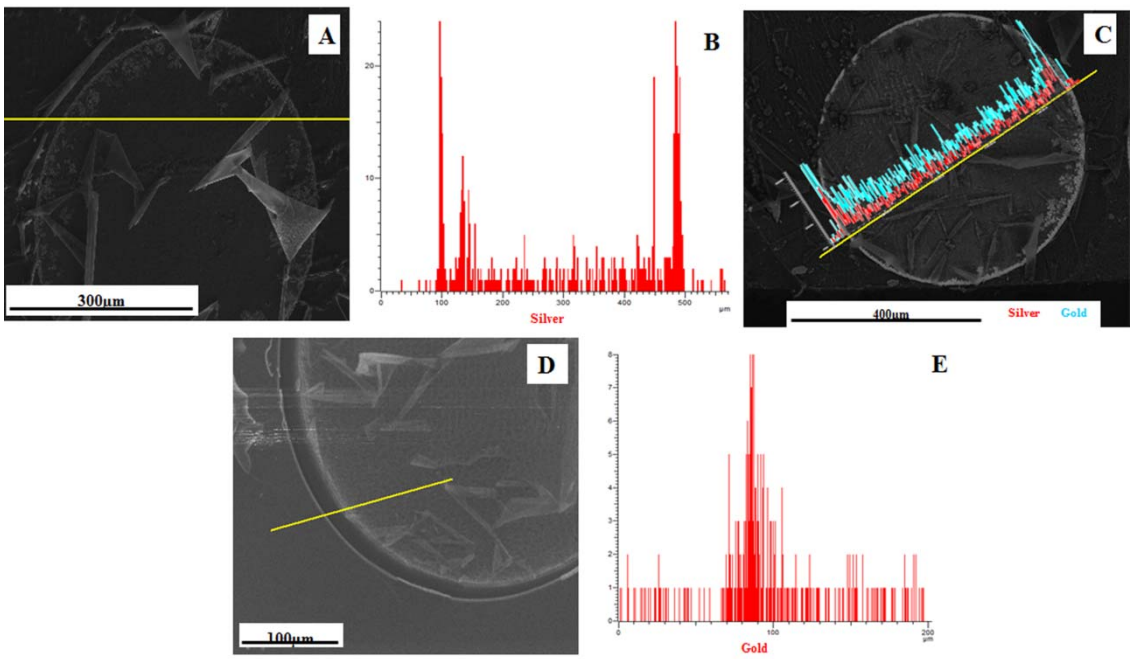

Figure 3: Cross-Section FE-SEM images with the corresponding EDS-LineScan mapping for Ag-FMNPs (A, B), AgAu-FMNPs (C) and Au-FMNPs on anion exchange resin.

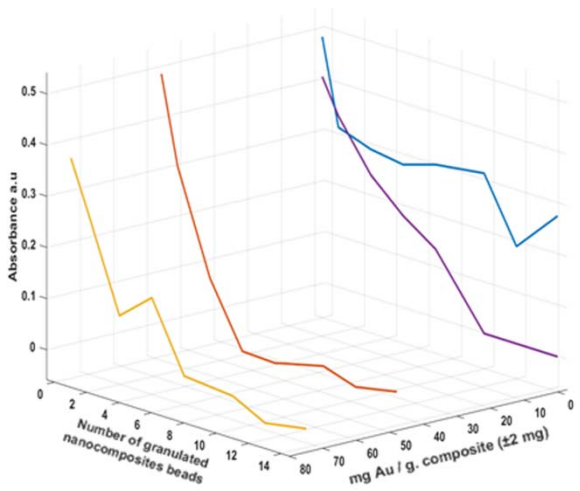

Figure 4: Inhibitory activity experiments for raw A520E resin (blue plot), Ag-FMNPs nanocomposite (purple plot), AgAu-FMNPs nanocomposite (red plot) and Au-FMNPs (yellow plot) as function of gold content in the final NC material

Au and AgAu-FMNPs containing NCs showed inhibitory activities with a decrease in the absorbance magnitude at 650 nm when increasing the number of granulated nanocomposite beads in the suspension and when increasing the Au content in the NC. In contrast, the raw material did not present significant inhibitory activity at this concentration range, with a constant absorbance value around 0.4 A.U. in all cases. These results indicated that Au-FMNPs content is proportional for the inhibition of *E. coli* bacteria proliferation. This information results a relative enhancement from the previously reported inhibitory activity of Ag-FMNPs on A520E resin.[39] Moreover, this proves unequivocally the feasibility of IMS to prepare novel bactericide NCs (mono or bimetallic) with different Au content.

Electrocatalytic effect of Ag-FMNPs and Au-FMNPs on electrochemical nanocomposite sensors

The feasibility of the IMS technique to incorporate Ag-FMNPs and Au-FMNPs on a nanostructured carbon material was studied, using MWCNTs as nanofiller material. The resulting hybrid-nanomaterials were the Ag-FMNPs@MWCNTs and the Au-FMNPs@MWCNTs. From Figure 5 it is possible to observe a favorable distribution of these FMNPs on the MWCNTs surface. In addition to the distribution of the FMNPs, it was also observed a homogenous size distribution over MWCNTs surface and no FMNPs agglomeration was detected. The possible aggregation of t NPs limits their application in electrochemical systems. Thus, their preparation by IMS provides an extra level of stability and a favourable distribution in the final nanocomposite material (as can be seen in Figure 5).

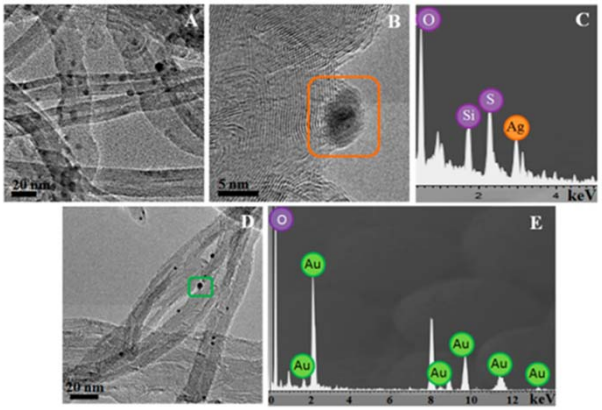

Figure 5: TEM images and EDS spectra for Ag-FMNPs@MWCNTs (A,B,C) and the Au-FMNPs@MWCNTs (D,E) showing the location of the FMNPs mainly on the surface of the MWCNTs.

Moreover, IMS is an environmentally friendly technique as it is carried out at room temperature, in aqueous solution and with low concentration of reagents. Other techniques used for the modification of CNTs with NPs usually involve more complex – time consuming processes such as thermal evaporation, electroless deposition by galvanic replacement, MNPs hydrosol absorption or electrochemical deposition.[12]

The quantification of the metal content on the MWCNTs walls was carried out by TGA. The residue at the end of analysis corresponds to the total metal content. The amount of metal impurities of raw MWCNTs after acidic treatment was 2% in catalyst. When the different kinds of FMNPs@MWCNTs were analyzed, this 2% of catalyst remaining was subtracted in order to quantify the FMNPs content. Accordingly to TGA analysis, an amount of 5.6% and 6.6% in FMNPs was observed for Ag–FMNPs@MWCNTs and Au–FMNPs@MWCNTs, Drespectively. It is important to emphasize that TGA provides only quantitative information on the presence of total metal content in CNT material. Under this context, EDS analysis is needed for the qualitative determination of the metal composition. As can be observed in Figure 5 (C and D), EDS is a successful tool to differentiate the FMNPs attached on the MWCNTs walls from the catalyst remaining from the industrials synthesis of the raw MWCNTs.

Afterwards, the effect of MWCNTs surface modification with Ag–FMNPs and Au–FMNPs on the electrochemical response of MWCNT-based nanocomposite electrodes was studied by EIS. For this aim, the Au–FMNPs@MWCNTs and Ag–FMNPs@MWCNTs were used as conducting nanofiller material and dispersed within an insulating polymeric matrix (the epoxy resin) for nanocomposite electrodes fabrication. It is important to highlight that 10% w/w in conducting nanofiller material was used as optimum composition ratio, accordingly with previous results.[35] Their results were also compared with the electrodes containing raw MWCNTs. Impedimetric studies are depicted in Figure 6. Nyquist plots show an optimum kinetically controlled response for these electrodes based on FMNPs@MWCNTs/epoxy nanocomposites. In addition, it is also possible to observe a higher decrease on the charge transfer resistance (R_{ct}) value when the amount of FMNPs

Table 1: Electrochemical (R_Ω, R_{ct} and C_{dl}) and electroanalytical (LOD, lineal range and sensitivity) comparative study using different types nanocomposite sensors based on MWCNT modified (Au-NPs@MWCNTs/epoxy and Ag-NPs@MWCNTs/epoxy nanocomposite) or not modified (raw MWCNTs/epoxy nanocomposite).

Sensor containing	Electrochemistry			Amperometry		
	R_Ω (Ω)	R_{ct} (Ω)	C_{dl} (μF)	LOD ($mg \cdot L^{-1}$)	Lineal Range ($mg \cdot L^{-1}$)	Sensitivity ($\mu A \cdot L \cdot mg^{-1}$)
Raw MWCNTs	138.0	530.0	9.02	0.070 ± 0.004	0.11–1.1	0.022 ± 0.003
Ag-FMNPs@MWCNTs	137.6	287.5	7.89	0.007 ± 0.002	0.028–1.3	0.029 ± 0.003
Au-FMNPs@MWCNTs	137.8	192.1	6.93	0.007 ± 0.002	0.014–1.7	0.058 ± 0.009

incorporation on the MWCNTs surface increases. Since this parameter is inversely proportional to the electron transfer rate, if the conductor material load increases, the probability of having more electroactive sites increases, as well as the electrode kinetics. Accordingly, electrodes containing Au–FMNPs (6.6% by TGA) presented a higher decrease of R_{ct} than those containing Ag–FMNPs (5.6% by TGA), as can be observed in Table 1.

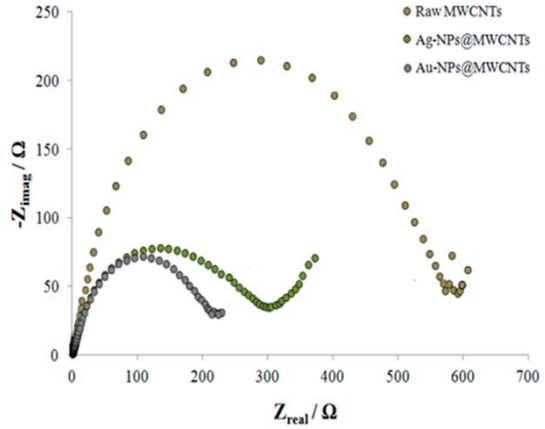

Figure 6: Nyquist plots of nanocomposite sensors based on MWCNT modified (Au-NPs@MWCNTs/epoxy and Ag-NPs@MWCNTs/epoxy nanocomposite) or not modified (raw MWCNTs/epoxy nanocomposite). The experiments were carried out in a 0.1 M KCl solution containing 0.01 M $[Fe(CN)_6]^{3-/4}$

Regarding ohmic resistance (R_Ω) parameter, from Table 1 it is possible to observe a slight decrease of R_Ω for FMNPs@MWCNTs/epoxy nanocomposite electrodes respect to the ones non-modified (raw MWCNTs). This is because the R_Ω is more controlled by the solution resistance for nanocomposites containing a higher load of conductor material.

The fact that nanocomposite electrodes with low charge resistances (R_Ω and transfer resistance (R_{ct})) are more appropriate to be used in electroanalytical measurements suggests that the use of nanocomposites containing FMNPs guarantees fast electron exchange. However, the enhanced kinetics is usually accompanied by an increase of the background current. As a consequence, it is important to consider the remaining impedance parameter represented by the capacitance of double layer value (C_{dl}). This parameter is directly related to the charge or background current and, consequently with the achieved detection limit. In general, C_{dl} parameter exhibits higher values for electrodes with higher amount of conducting material. However, when FMNPs are incorporated on MWCNTs surface, their electrocatalytic effect causes a significant decrease of the C_{dl} value (19% for electrodes containing Ag–FMNPs@MWCNTs and 23% for the ones containing Au–FMNPs@MWCNTs), as can be also observed in Table 1.

Accordingly, this functionalization improves different electrochemical properties that should allow the electrodes to enhance some analytical parameters, such as lineal range, sensitivity and detection limits. As proof of concept, the final electrocatalytical effect of Ag–FMNPs and Au–FMNPs as modifiers of MWCNTs on the oxidation of ascorbic acid, which was used as a model analyte, has been studied in this work. For this aim, the MWCNTs tuned with Ag–FMNPs and Au–FMNPs were used for development of working electrodes based on MWCNTS/epoxy nanocomposite electrodes. The obtained results were compared with those obtained by the raw MWCNTs/epoxy nanocomposite sensor.

The electroanalytical response of these modified-sensors was carried out by hydrodynamic amperometry for the oxidation of ascorbic acid (E_{app}= +0.60 V *vs.* Ag/AgCl; constant stirring). Several analytical parameters, such as limit of detection (LOD), limit of quantification (LOQ), sensitivity and lineal range were evaluated. LOD was estimated three times by the N/S=3 criterion[12]. The calibration curves for ascorbic acid oxidation are depicted in Figure 7.

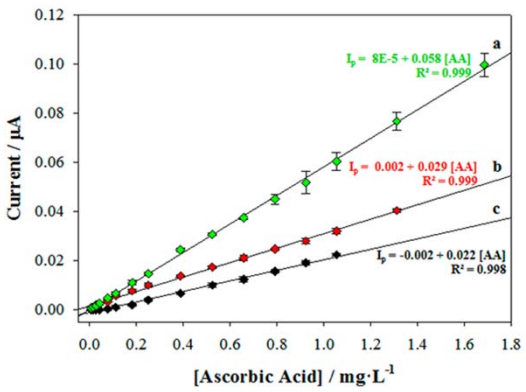

Figure 7: Calibration curves of Ip vs. concentration of ascorbic acid (AA) for nanocomposite sensors containing a) Au–FMNPs@MWCNTs, b) Ag–FMNPs@MWCNTs and c) raw MWCNTs. Values are represented with their corresponding error bars (n=3). The experiments were carried out in a in a 0.01 M KNO3/HNO3 solution

If the raw MWCNT/epoxy nanocomposite sensor demonstrated a great response for the detection of ascorbic acid in water, the nanocomposite sensors containing FMNPs exhibited a superb enhanced of its response, also accompanied by an electrocatalytic effect, as is shown in Table 1. This fact results in a decade of concentration less in the LOD for ascorbic acid determination. As can be easily observed from Figure 7, better sensitivities and wider lineal ranges were obtained when sensors were modified with FMNPs, obtaining a higher sensitivity using the Au–FMNPs@MWCNTs/epoxy nanocomposite sensor (see Table 1). This fact might be explained due to there is a higher amount of electrocatalytic nanoparticles (0.66% of Au–FMNPs *vs.* 0.56% of Ag–FMNPs) in the nanocomposite sensor.

Accordingly, thanks to the electrocatalytic effect of the FMNPs presented on the nanocomposite electrodes, the developed functionalized sensors exhibit the characteristics that an electrode must have, such as high sensitivity, low LOD and fast response time.

Conclusions

Intermatrix Synthesis technique has proved to be a suitable synthetic methodology for the preparation of nanocomposites with tuned nanoparticle distribution depending on the reducing agent used; proving that Donnan Effect has a determinant role during the nanoparticles appearance. Moreover, the composition of these nanoparticles can be customized by coupling a galvanic replacement stage to Intermatrix Synthesis in order to obtain Au- and AuAg-FMNPs containing nanocomposites; mainly located near the surface of the resin bead. This fact is advantageous for specific applications, such as successfully tested in E.coli inhibitory activity assays; seemingly be associated with the Au content in the nanocomposite beads.

In addition, the feasibility of Ag–FMNPs and Au–FMNPs in multiwall carbon nanotubes based nanocomposite sensors was electrochemically studied, obtaining enhanced electrochemical parameters after the incorporation of the nanoparticles, such as lower resistances and higher signal-to-noise ratios. These improvements were verified in terms of electroanalytical response, using ascorbic acid as a model analyte. The functionalized-nanocomposite sensors showed excellent analytical parameters for the oxidation of ascorbic acid, resulting in better Limits of Detection and higher sensitivities regarding to the non-modified electrodes, which is mainly thanks to the electroanalytical properties of the functional metal nanoparticles.

Acknowledgements

Programa Operatiu de Catalunya (FEDER) is acknowledged for the financial support within the project VALTEC09-02-0058. This work was partially funded by the MINECO projects CTQ2014-54553-C3-2-R and CTQ2014-61809-EXP. JB and JM also thank Universitat Autònoma de Barcelona for the personal grants during PhD studies and Servei de Microscòpia of the Universitat Autònoma de Barcelona for the assistance for electron microscopy images.

References

1 V. Polshettiwar and R. S. Varma, *Green Chem.*, 2010, **12**, 743.
2 N. Elizondo, P. Segovia and V. Coello, in *Green Chemistry - Environmentally Benign Approaches*, ed. M. Kidwai, InTech, 2012.
3 S. Iravani, *Green Chem.*, 2011, **13**, 2638.
4 J. M. Campelo, D. Luna, R. Luque, J. M. Marinas and A. a Romero, *ChemSusChem*, 2009, **2**, 18–45.
5 Y. Xiao and C. M. Li, *Electroanalysis*, 2008, **20**, 648–662.
6 N. Savage, M. S. Diallo, J. Duncan, A. Street and R. Sustich, *Nanotechnology Applications for Clean Water*, William Andrew Inc, Nueva York, First., 2009.
7 L. Nicolais and G. Carotenuto, *Metal-polymer nanocomposites*, A JOHN WILEY & SONS, INC, New Jersey, 2005.
8 U. Ozkan, *Design of heterogeneous catalysts*, Wiley-VCH Verlag GmbH & Co. KGaA, 2009.
9 P. Ruiz, M. Muñoz, J. Macanás, D. N. Muraviev, M. Muñoz, J. Macanás, D. N. Muraviev, M. Muñoz, J. Macanás and D. N. Muraviev, *Chem. Mater.*, 2010, **22**, 6616–6623.
10 J. Bastos-Arrieta, A. Shafir, A. Alonso, M. Muñoz, J. Macanás and D. N. Muraviev, *Catal. Today*, 2012, **193**, 207–212.
11 J. Muñoz, F. Cespedes and M. Baeza, *J. Electrochem. Soc.*, 2015, **162**, B217–B224.
12 J. Muñoz, J. Bastos-Arrieta, M. Muñoz, D. N. Muraviev, F. Céspedes and M. Baeza, *RSC Adv.*, 2014, **4**, 44517–44524.
13 S. Li, Y. Zheng, G. W. Qin, Y. Ren, W. Pei and L. Zuo, *Talanta*, 2011, **85**, 1260–1264.
14 M. Yang, Y. Yang, Y. Liu, G. Shen and R. Yu, *Biosens. Bioelectron.*, 2006, **21**, 1125–31.
15 Y. Liu, Z. Su, Y. Zhang, L. Chen, T. Gu, S. Huang, Y. Liu, L. Sun, Q. Xie and S. Yao, *J. Electroanal. Chem.*, 2013, **709**, 19–25.
16 C. Bittencourt, a. Felten, J. Ghijsen, J. J. Pireaux, W. Drube, R. Erni and G. Van Tendeloo, *Chem. Phys. Lett.*, 2007, **436**, 368–372.
17 H. C. Choi, M. Shim, S. Bangsaruntip and H. Dai, *J. Am. Chem. Soc.*, 2002, **124**, 9058–9.
18 K. Y. Lee, M. Kim, J. Hahn, J. S. Suh, I. Lee, K. Kim and S. W. Han, *Langmuir*, 2006, **22**, 1817–21.
19 L. Qu, L. Dai and E. Osawa, *J. Am. Chem. Soc.*, 2006, **128**, 5523–32.
20 J. Bastos-Arrieta, J. Muñoz, A. Stenbock-Fermor, M. Muñoz, D. N. Muraviev, F. Céspedes, L. A. Tsarkova and M. Baeza, *Appl. Surf. Sci.*, 2016, **368**, 417–426.
21 D. N. Muraviev, *Contrib. to Sci.*, 2005, **3**, 19–32.
22 P. Ruiz, M. Muñoz, J. Macanás and D. N. Muraviev, *Chem. Mater.*, 2010, **22**, 6616–6623.
23 J. Bastos-Arrieta, M. Muñoz, P. Ruiz and D. N. Muraviev, *Nanoscale Res. Lett.*, 2013, **8**, 255.
24 P. Ruiz, J. Macanás, M. Muñoz and D. N. Muraviev,

Nanoscale Res. Lett., 2011, **6**, 343.
25 P. Ruiz, M. Muñoz, J. Macanás, C. Turta, D. Prodius and D. N. Muraviev, *Dalton Trans.*, 2010, **39**, 1751–7.
26 B. Domènech, M. Muñoz, D. N. Muraviev and J. Macanás, *Nanoscale Res. Lett.*, 2011, **6**, 406.
27 A. Alonso, N. Vigués, X. Muñoz-Berbel, J. Macanás, M. Muñoz, J. Mas and D. N. Muraviev, *Chem. Commun. (Camb).*, 2011, **47**, 10464–6.
28 J. Bastos-Arrieta, M. Muñoz and D. N. Muraviev, *Solvent Extr. Ion Exch.*, 2014, **33**, 152–165.
29 N. R. Sieb, N. Wu, E. Majidi, R. Kukreja, N. R. Branda and B. D. Gates, 2009, **3**, 1365–1372.
30 T. K. Sau and A. L. Rogach, *Adv. Mater.*, 2010, **22**, 1781–804.
31 C. M. Welch and R. G. Compton, *Anal. Bioanal. Chem.*, 2006, **384**, 601–19.
32 J. Muñoz, M. Riba-Moliner, L. J. Brennan, Y. K. Gun'ko, F. Céspedes, A. González-Campo and M. Baeza, *Microchim. Acta*, 2016.
33 M. D. Adhikari, S. Goswami, B. R. Panda, A. Chattopadhyay and A. Ramesh, *Adv. Healthc. Mater.*, 2013, **2**, 599–606.
34 Y. Cui, Y. Zhao, Y. Tian, W. Zhang, X. Lü and X. Jiang, *Biomaterials*, 2012, **33**, 2327–33.
35 J. Muñoz, J. Bartroli, F. Céspedes and M. Baeza, *J. Mater. Sci.*, 2014, **50**, 652–661.
36 M. L. Personick and C. a Mirkin, *J. Am. Chem. Soc.*, 2013, **135**, 18238–47.
37 L. Suber, I. Sondi, E. Matijević and D. V Goia, *J. Colloid Interface Sci.*, 2005, **288**, 489–95.
38 D. Goia, *New J. Chem.*, 1998, 1203–1215.
39 A. Alonso, X. Muñoz-Berbel, N. Vigués, R. Rodríguez-Rodríguez, J. Macanás, J. Mas, M. Muñoz and D. N. Muraviev, *RSC Adv.*, 2012, **2**, 4596–4599.
40 L. Cumbal and A. K. Sengupta, *Environ. Sci. Technol.*, 2005, **39**, 6508–15.
41 P. Puttamraju and A. K. SenGupta, *Ind. Eng. Chem. Res.*, 2006, **45**, 7737–7742.
42 R. Levenstein, D. Hasson and R. Semiat, *J. Memb. Sci.*, 1996, **116**, 77–92.
43 W. Wang, M. Dahl and Y. Yin, *Chem. Mater.*, 2012, **25**, 1179–1189.
44 B. Domènech, M. Muñoz, D. N. Muraviev and J. Macanás, *Chem. Commun. (Camb).*, 2014, **50**, 4693–5.